

Christopher D. Torres¹, Alexandra M. Boyat², Vivekananda P. Adiga³, Anirudha V. Sumant⁴,
Robert W. Carpick⁵, Frank E. Pfefferkorn⁶

¹Christopher D. Torres; Mechanical Engr., University of Wisconsin-Madison, USA; cdtorres@wisc.edu

²Alexandra M. Boyat; Mechanical Engr., University of Wisconsin-Madison, USA; boyat@wisc.edu

³Vivekananda P. Adiga; Materials Science and Engineering, University of Pennsylvania, USA; adiga@seas.upenn.edu

⁴Anirudha V. Sumant; Center for Nanoscale Materials, Argonne National Laboratory, USA; sumant@anl.gov

⁵Robert W. Carpick; Mechanical Eng. & Applied Mechanics, University of Pennsylvania, USA; carpick@seas.upenn.edu

⁶Frank E. Pfefferkorn; Mechanical Engr., University of Wisconsin-Madison, USA; pfefferk@engr.wisc.edu*

INTRODUCTION

The demand for the miniaturization of complex components has led to the growth of manufacturing methods capable of producing truly three dimensional parts using traditional engineering materials with favorable mechanical properties. Mechanical micromachining techniques have emerged for the production of these components as other methods are not capable of producing many of the desired component properties. Micro end milling is one such mechanical micromachining technique. It is able to produce three-dimensional features with high aspect ratios from various materials, such as aluminum, copper, steel, and titanium [1-2]. Currently, the standard material used for micro end mill tooling is sintered tungsten carbide with a cobalt binder [2-3]. However, its brittle nature coupled with the micro-scale cutting features of the end mills often result in rapid tool degradation [1]. Soft, ductile materials tend to adhere to the tool cutting surface, easily clogging the micro-sized flutes. This results in high cutting forces and force spikes, drastically reducing the tool life [4]. On the other hand, hard materials tend to increase the abrasive wear rate on the tool cutting edges or cause catastrophic edge failures [1]. Micro end mills typically experience much higher wear rates when compared to macro-sized end mills due to the relative size of the chip load compared to the cutting edge radius of the tool and the overall size of the tool [1, 5]. Due to this fundamental difference during the cutting process, many of the wear characteristics and tool life knowledge for conventional tooling may not apply to micro end milling [1, 6-8]. Even many of the standards developed to determine tool life and tool wear cannot be applied for micro end mill testing because they are based on the typical cutting parameters and chip loads for macro scaled milling operations [9]. As such, micro end milling production has been severely limited because of the amount of "guess work" surrounding tool life. This study will investigate tool life and wear of nanocrystalline diamond (NCD) coated and uncoated tungsten carbide (WC) micro end mills during milling of 6061-T6 aluminum.

EXPERIMENTAL PROCEDURE

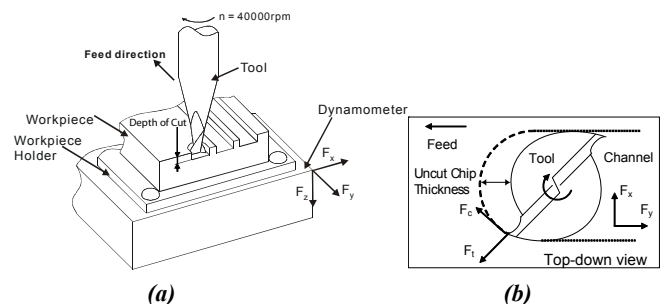
Commercially available, 305 μm diameter, 2-flute end mills (PMT part TS-2-0120-S) were used throughout the study. The end mill tool life and wear rates were compared between

three standard, as-received WC end mills and three nanocrystalline diamond (NCD) coated end mills. The NCD coatings were produced with a hot-filament chemical vapor deposition (HF-CVD) procedure [10]. The sensitivity of the HF-CVD process resulted in variations in the diamond coating thicknesses: 450 nm, 270 nm, and 190 nm.

Fig. 1 illustrates the test setup used for the machining experiments. A high-speed spindle (NSK-HES500) with electric drive and ceramic bearings was mounted to the spindle of a CNC milling machine (HAAS TM-1). A constant spindle speed of 40,000 rpm and feed rate of 250 mm/min were used to dry mill full-width slots in 6061-T6 aluminum for all of the experiments (Table 1).

Forces acting on the workpiece were measured by a three-axis force dynamometer (Kistler 9256C2). The dynamometer was able to dynamically measure the cutting forces in the x , y and z axes. LabView software and National Instruments data acquisition hardware (NI PCI 6014) were used to record the force data at a rate of 60 kHz. Both uncoated and coated tools were tested in the same batch to ensure compatibility. A humidity control system was used to maintain a constant relative humidity of approximately 85% at the tool-workpiece interface.

The machining conditions used are shown in Table 1. The tests consisted of dry machining a single full-width channel 50 mm long and 45 μm deep, in a 50 mm \times 50 mm \times 4.8 mm 6061-T6 aluminum block. The workpiece was mounted on the dynamometer before its surface was prepared by facing with a one inch end mill to ensure flatness within 3 μm . Each tool was fixed in the high speed spindle and then aligned to the workpiece using an optical magnification system. The alignment uncertainty was $\pm 5 \mu\text{m}$ in the z -axis.



* corresponding author

Fig. 1. Schematic of micro end milling: (a) 3D view of the experimental setup, (b) end view of the cutting process.

Table 1: Milling parameters

Workpiece Material	6061-T6 Aluminum
Temperature / R.H.	~23°C / ~85%
Tool (end mill):	PMT Model TS-2-0120-S
Material	0.4 μm grain WC-Co
Diameter	305 μm (0.012 in.)
Flutes	2
Helix	30°
Coating	190-450 nm NCD or None (bare WC)
Spindle Speed	40,000 rpm
Feed	250 mm/min
Chip Load	3.125 μm
Depth of Cut	45 \pm 5 μm
Width of Cut	300 \pm 2 μm

End mills were inspected for defects and the diameter and cutting edge radii were measured before testing to ensure consistent quality between tools. The uncoated end mills were inspected after linear cutting distances of 50, 50, 50, 100, 150, 1000, and 1000 mm for a total length of 2.4 m. It should be noted, that the third uncoated tool was not tested for the final 1 m due to testing limitations, and not because the tool had fractured. The NCD coated tools were inspected after linear cutting distances of 50, 50, 50, 100, 1000, and 1000 mm for a total length of 2.25 m.

After milling, the tools were ultrasonically treated in sodium hydroxide in order to remove any adherent aluminum from the flutes and cutting edges of the tool. Unfortunately, this removal of aluminum will result with clean cutting edges and flutes on the tool that will affect cutting performance and tool life.

Tool wear was evaluated by comparing both the change in tool tip edge radius along with the change in overall tool diameter on the end mill via scanning electron microscopy (Leo 1530 field emission scanning electron microscope). The tool diameter was measured by drawing the largest centric circle that encompasses the entire tool. Fig. 2a illustrates the diameter measurement taken on an uncoated end mill. The tool tip radius was determined by drawing a circle that would capture the curvature of the cutting edge at the cutting tips of the tool. Fig. 2b shows an example of the cutting edge radius measurement on one of the tool tips of an NCD coated end mill.

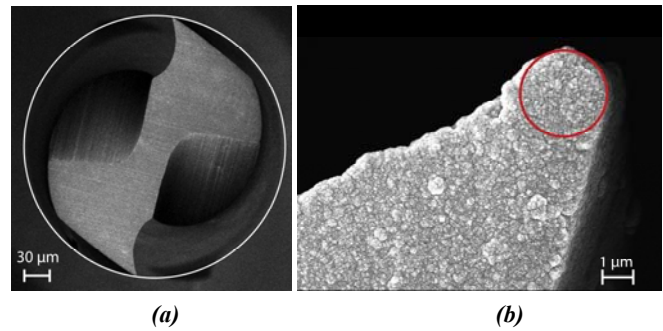


Fig. 2. Examples of wear measurements: (a) end mill diameter measurement, (b) cutting edge radius measurement.

Viewing the end of the tool, the height of the cutting edges with respect to the center of the tool (Fig. 3) were measured with a white light interferometer (Zygo NewView 6400). The height is determined by calculating the largest vertical distance between the center of the tool and the cutting tips. The average height difference between the two tips was then averaged together, as the low magnification of the instrument makes it difficult to track each of the tips individually throughout the experiments.

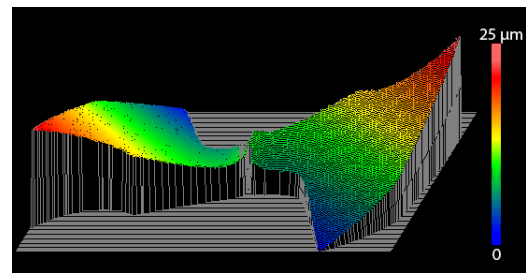


Fig. 3. Examples of height measurement using white light interferometry.

Milled channels were also analyzed using the white light interferometer. Changes in roughness, channel width, and the formation of burrs were quantified. Finally, cutting forces were collected throughout the experiment to determine a correlation between the forces and changes in the cutting edge condition.

RESULTS

A. TOOL WEAR MEASUREMENTS

The initial wear on the tools is largely a function of how long the sharp cutting edges are able to survive before fracturing. Very little wear is observable on the tool edges up to the fracture of the tool tips. After fracture the effective tool diameter is significantly reduced. In addition, the fracturing of the tips changes the cutting edge geometry and potentially results in an effective negative rake angle, depending on the chip load (Fig. 4a). Continuing to cut with the tool results in wear that rounds off the leading edge of the fractured surface (Fig. 4b). After approximately 500 mm of cutting, the tool diameter stabilizes with little additional wear measured based on the tool diameter metric (Fig. 5).

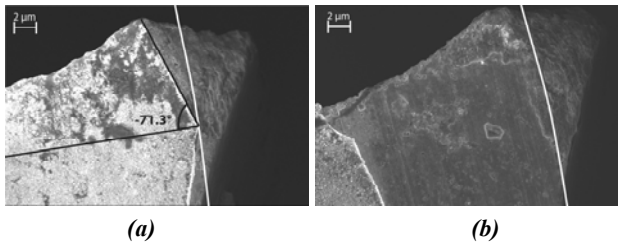


Fig. 4. Coated end mill cutting edge that shows: (a) formation of negative rake angle after edge fracture after 100 mm of milling, and (b) wearing of negative rake angle after 150 mm of milling.

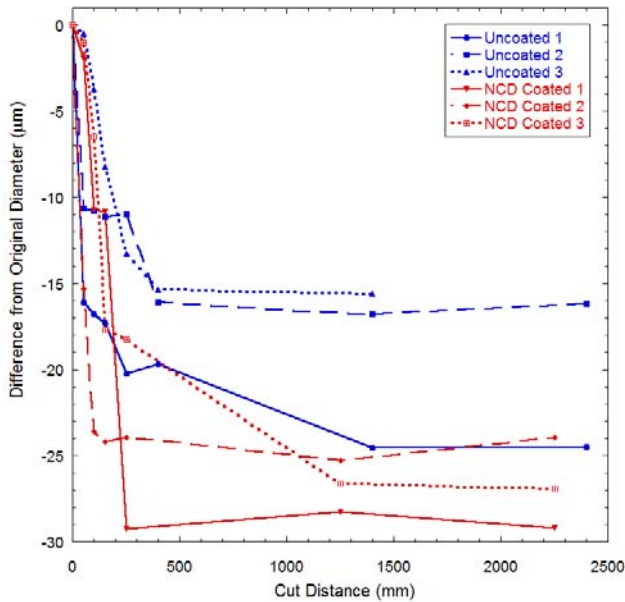


Fig. 5. Change in diameter comparison from the original diameter of each of the six tools.

When comparing the wear between the NCD coated and bare WC tooling, there is evidence that the diamond coating preserves the initial tool geometry longer than the uncoated tools (Fig. 6). The NCD coated tools show very little evidence of wear initially and produce a good surface finish. However, surface preparation required for NCD coating removes surface cobalt in order to improve diamond synthesis on the tool. This removal of cobalt results in a loss of fracture toughness of the tool. As a result, when the tip of a NCD coated tool does fracture, a larger piece of the cutting edge is lost as compared with the bare WC end mills (Fig. 7).

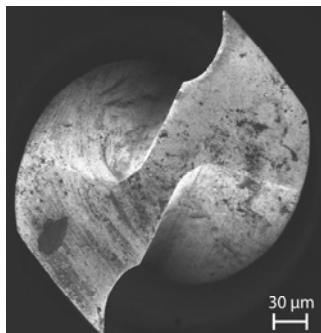


Fig. 6. An NCD coated end mill after 50 mm of milling indicating no edge fracture.

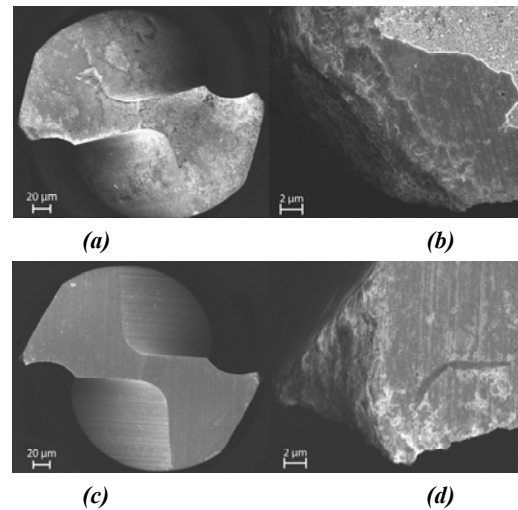


Fig. 7. Comparison of: (a) an NCD coated end mill after initial cutting edge fracture, (b) an NCD coated cutting edge after fracture, (c) a bare WC end mill after cutting edge fracture, and (d) a bare WC cutting edge after fracture.

Fig. 5 shows that there are two outliers, NCD coated tool #2 and uncoated tool #3, that conflict with the stated initial wear benefits with the NCD coatings. The large wear found with NCD coated tool #2 is an artifact of the experimental resolution. In fact, based on the force measurements taken for each of the tools, the first major location of edge failure (indicated by a sudden increase in forces) for the uncoated tools all occurred within the first 100 μm of milling. The NCD coated tools did not fail until 52 mm, 6.8 mm, and 36.8 mm of milling, respectively (Fig. 8). Since the initial cut distance was set at 50 mm, these benefits would not be captured within the wear measurements.

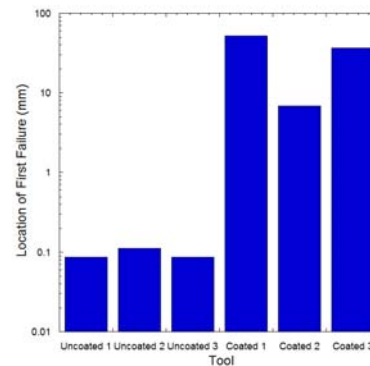


Fig. 8. Comparison of cut distance before the first apparent cutting edge fracture.

The change in height of the tool tips are given in Fig 9. Measurements beyond a cutting distance of 500 mm are not plotted due to very little geometric change occurring with the tools, and to allow easier visibility of the changes occurring within initial cuts. The measurements and conclusions determined from the tool diameter measurements are further reinforced by the height measurements. NCD coated tools tend to produce very little change early on in testing, until they reach a critical fracture point where there is a significant change in height because of the larger amount of material lost

during the fracture event. After fracturing, additional wear occurs on the tools until a stable cutting geometry is developed. Unlike the diameter measurement, all three uncoated measurements indicate higher initial wear than the NCD tools, with the exception of NCD tool #3. After the initial wear, the uncoated tools enter into a stable geometric régime with lower overall wear compared to the NCD tools. One thing to note with this measurement is that due to the sample orientation on the white light interferometer stage, there is an overall measurement error of approximately $0.4 \mu\text{m}$. In the worst wear case, NCD coated tool #3 after 250 mm of cutting distance, the measurement uncertainty is 15%. The uncertainty is greater at smaller values of wear, suggesting that this is not the most suitable wear measurement metric for micro end mills.

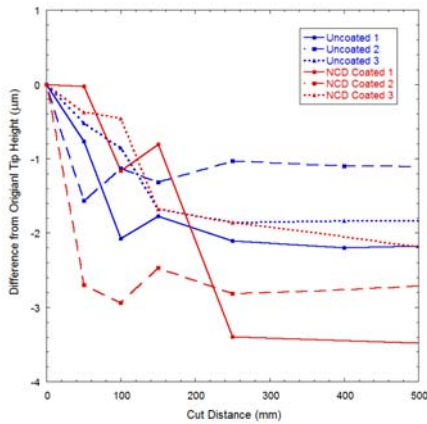


Fig. 9. Average change in tool height from the original tool height of each of the six tools.

Measuring changes in the cutting edge radius as wear progressed was challenging because of the significant change in the cutting edge geometry after tip fracture. The blunting of an edge during cutting could be measured, however, identifying and measuring the cutting edge radius after fracture requires further investigation. In addition, correlating the cutting edge radius and effective rake angle with cutting forces and surface finish is part of ongoing research.

B. REDUCTION OF CUTTING AND THRUST FORCES

Average measured maximum cutting and thrust forces for 10 tool rotations for each tool are shown in Fig. 10 for seven different cutting distances. For the initial cutting section, $<100 \mu\text{m}$, the average cutting and thrust forces for the bare WC end mills are less than the forces measured for the NCD coated end mills. Since the tool edges have not fractured at this point, it is believed that the lower forces of the bare end mills are a result of smaller cutting edge radius. The uncoated end mills had an average cutting edge radius of 752 nm , while the NCD coated end mill had an average radius of 1393 nm . Given the small chip load, $3.125 \mu\text{m}$, the size of the cutting edge radius can significantly impact the effective rake angle, hence the magnitude of the cutting forces.

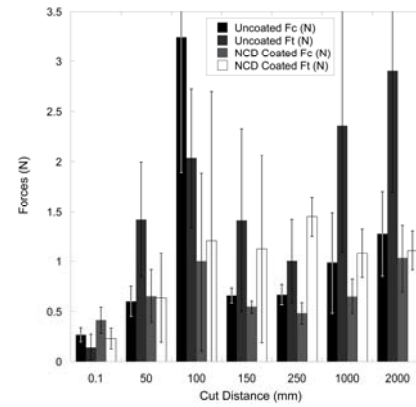


Fig. 10. Average cutting and thrust forces for coated and uncoated tools at 7 different cut distance intervals.

At a cut distance of 50 mm, the uncoated tools exhibit a much higher thrust force. This is a direct result of the edges fracturing and creating an effective negative rake angle tool. Depending on how well the cutting edges of the NCD coated tools are maintained throughout milling, the forces remained relatively low and balanced, which indicates that the material removal is largely done from chip formation and removal as opposed to ploughing and grinding. At approximately 100 mm linear cutting distance, all of the cutting edges have fractured on all of the tools. At this point, the newly fractured tool edges created smaller and negative effective rake angles resulting in larger cutting forces. However, this geometry is not optimal or stable and is slowly worn away resulting in an improved cutting geometry. This results in a lowering of the cutting forces at further milling distances. The tools continue to wear until they reach a stable cutting geometry, where they are strong enough to withstand any additional cutting edge fracture and concentric enough to reduce the abrasive wear occurring on the flank face of the tools (Fig. 11). At this point, the tools contain a positive rake angle and large cutting edge radius geometry. This causes higher thrust forces measured at the higher milling distances. After 2 m of milling, the uncoated tools had an average radius of $1.7 \mu\text{m}$, while the coated tools had an average radius $5.6 \mu\text{m}$.

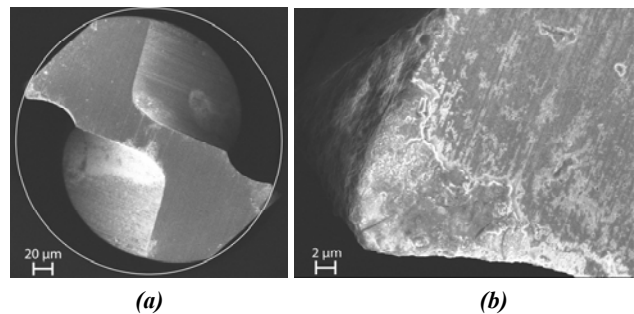


Fig. 11. (a) Cutting diameter of uncoated tool after 1 m milling, and (b) cutting edge of uncoated tool after 1 m milling.

Even though the coated tool edges tend to also fracture within the first 100 mm of milling, the tool forces are generally lower throughout the rest of the tests. Further analysis of the tools after 2 m of milling indicates that there is still NCD present within the flutes of the coated end mills (Fig. 12).

The lower forces can therefore be attributed to the lower adhesion and friction between the chips and the NCD coating. This prevents clogging of the flutes and lowers the forces acting on the end mills.

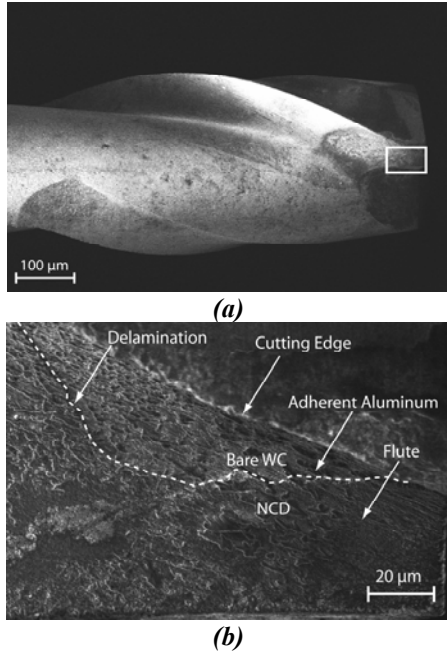


Fig. 12. (a.) Side profile of NCD coated end mill after 2 m of milling, and (b) magnified image of cutting edge and flute showing NCD present within the flute of the end mill.

C. WORKPIECE SURFACE FINISH

One goal of the wear analysis is to determine how long a micro end mill is able to produce an acceptable surface finish and feature tolerance. In addition, post processing procedures, such as deburring, play an important role in part development and cost. Because of this, surface analysis was performed on the channels produced during the wear testing.

During the initial milling both the uncoated and NCD coated tools produced rather clean and a highly uniform surface finish. However, the additional mechanical and tribological properties of the NCD coated surfaced resulted in significantly less burring when compared to the uncoated tool (Fig. 13).

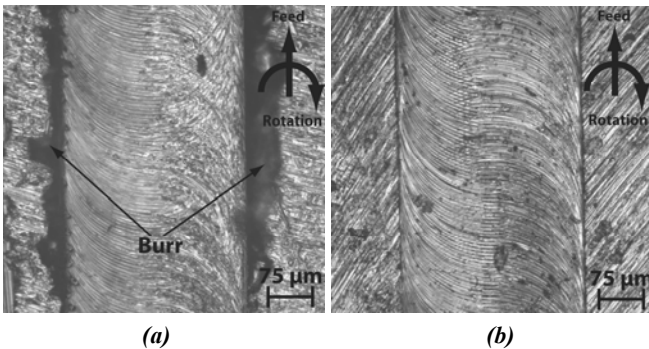


Fig. 13. Intensity profiles of the channels milled for (a) bare WC end mills, and (b) NCD coated end mills within the first 100 µm of cutting distance.

As milling continued, the condition of the milled channels for the uncoated tools continued to worsen with considerably more burring evident. In addition, the channel surface finish became more sporadic with more evidence of material adhering to the cutting tool resulting in smearing of the surface (Fig. 14a). On the other hand, the NCD coated tool continued to produce high quality channels even after initial tool tip fracture and delamination had occurred. Fig. 14b, shows a relatively small amount of burring with a continued uniformity of the surface finish.

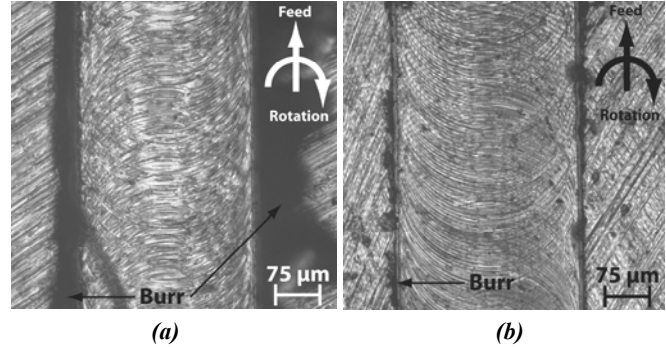


Fig. 14. Intensity profiles of the channels milled for (a) bare WC end mills, and (b) NCD coated end mills after 100 mm of cutting distance.

The uncoated surface finish did not improve as the tool geometry stabilized as milling continued. A large amount of burring is evident at the top edge of the milled channels (Fig. 15a). Burring also increased for the NCD coated tools, but the degree of burring still remained well below their uncoated counterparts (Fig. 15b).

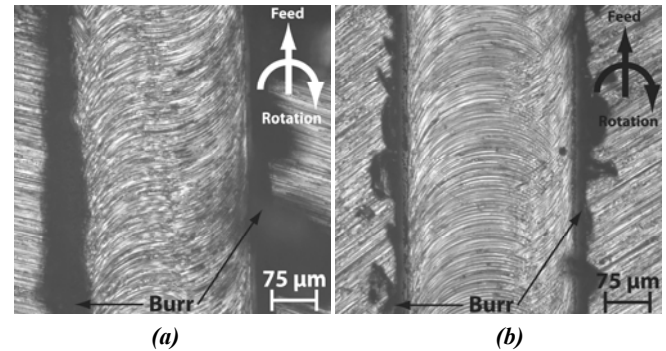


Fig. 15. Intensity profiles of the channels milled for (a) bare WC end mills, and (b) NCD coated end mills after 2 m of cut distance.

Roughness values of each of the channels were measured at 7 different cut intervals (Fig. 16). The measurements were taken via a line profile, 0.7 mm long, running down the center of the channel using a 10X magnification. Images were captured at a resolution of 640 x 480 pixels. Unlike the cutting forces or tool diameter the surface roughness measurements do not capture any discernable trends with respect to tool wear. The NCD coated tools produced a consistent average and RMS surface roughness throughout the 2 m of linear cutting distance, even after tool edge fracture and coating delamination had occurred. The uncoated tools, however, produced instances of significantly higher average and RMS

surface roughness (Fig. 16) which corresponded with significant edge fracture events. After the tool geometry had stabilized, for both NCD coated and bare WC tools, the NCD coated tools produced a smoother surface.

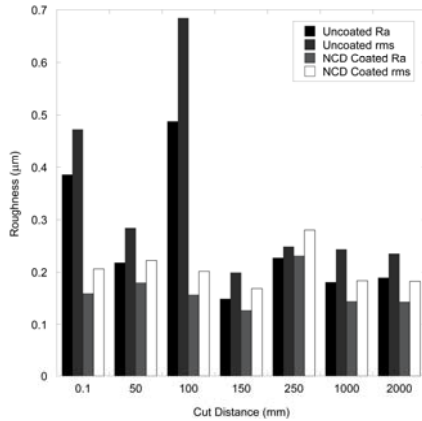


Fig. 16. Average Ra and rms roughness for the bare WC and NCD coated end mills at 7 different cut distance intervals.

Due to the burring in many of the channels, accurate measurements of the channels widths could not be made. In the near future, the channels will be deburred and channel widths measured to determine if there is a relationship between wear and tool runout.

CONCLUSIONS

For both NCD coated and bare WC micro end mills, initial tool wear is determined by the tool's ability to withstand cutting edge fracture early in the milling process. Once edge fracture occurs, the tool edge geometry changes and can produce a negative effective rake angle. Continued milling of the tool results in wear of the negative rake angle until a stable, positive rake angle, and relatively large edge radius, 1.7 µm for the uncoated and 5.6 µm for the coated tools, is produced. At this point, the rate of tool wear decreases significantly. The mechanical and tribological properties of the NCD coating allow increased milling duration before fracture. However, due to the removal of surface cobalt during diamond synthesis, a larger portion of the edge fractures from the tools, but continues to wear much like the uncoated end mills. Even after fracture and coating delamination near the cutting edge, the NCD coated tools still possesses an increased cutting performance, higher quality surface finish, and a reduced amount of burring when compared to the uncoated end mills.

ACKNOWLEDGMENTS

Support of this work by NSF Grants CMII-0700794 / 0700351, NSF supported shared facilities and the University of Wisconsin-Madison is gratefully acknowledged. Use of the Center for Nanoscale Materials at Argonne National Laboratory was supported by the U. S. Department of Energy, Office of Basic Energy Sciences, under Contract No. DE-AC02-06CH11357. The authors would like to thank Dave Burton from Performance Micro Tool for supplying micro end mills.

REFERENCES

- [1] X. Liu, R. E. DeVor, S. G. Kapoor, and K. F. Ehmann, "The Mechanics of Machining at the Microscale: Assessment of the Current State of the Science," *Journal of Manufacturing Science and Engineering*, vol. 126, 2004, pp. 666-678.
- [2] J. Chae, S. S. Park, and T. Freiheit, "Investigation of Micro-Cutting Operations," *International Journal of Machine Tools and Manufacture*, vol. 46, no. 3-4, 2006, pp. 313-332.
- [3] H. Sein, W. Ahmed, M. Jackson, R. Woodward, and R. Polini, "Performance and Characterisation of CVD Diamond Coated, Sintered Diamond and WC-Co Cutting Tools for Dental and Micromachining Applications," *Thin Solid Films*, vol. 447-448, 2004, pp. 455-461.
- [4] M. J. Jackson, G. M. Robinson, and W. Ahmed, "Micromachining Selected Metals using Diamond Coated Cutting Tools," *International Journal of Nanomanufacturing*, vol. 1, no. 2, 2006, pp. 304-317.
- [5] W. J. Endres, and R. K. Kountanya, "The Effects of Corner Radius and Edge Radius on Tool Flank Wear," *Journal of Manufacturing Processes*, vol. 4, no. 2, 2002, pp. 89-96.
- [6] C. J. Kim, M. Bono, and J. Ni, "Experimental Analysis of Chip Formation in Micro-Milling," *Transactions of NAMRI/SME*, vol. 30, 2002, pp. 247-254.
- [7] M. P. Vogler, S. G. Kapoor, and R. E. DeVor, "On the Modeling and Analysis of Machining Performance in Micro-Endmilling, Part II: Cutting Force Prediction," *Journal of Manufacturing Science and Engineering*, vol. 126, no. Copyright 2005, IEE, 2004, pp. 695-705.
- [8] M. P. Vogler, R. E. DeVor, and S. G. Kapoor, "On the Modeling and Analysis of Machining Performance in Micro-Endmilling, Part I: Surface Generation," *Journal of Manufacturing Science and Engineering*, vol. 126, 2004, pp. 685-694.
- [9] ISO, "Tool Life Testing in Milling - Part 2: End Milling," 1989.
- [10] P. J. Heaney, A. V. Sumant, C. D. Torres, R. W. Carpick, and F. E. Pfefferkorn, "Diamond Coatings for Micro End Mills: Enabling the Dry Machining of Aluminum at the Micro-Scale," *Diamond and Related Materials*, vol. 17, no. 3, 2008, pp. 223-233.